Genome rearrangements caused by interstitial telomeric sequences in yeast

Anna Y. Aksenova[a], Patricia W. Greenwell[b], Margaret Dominska[b], Alexander A. Shishkin[a], Jane C. Kim[a], Thomas D. Petes[b,1], and Sergei M. Mirkin[a,1]

[a]Department of Biology, Tufts University, Medford, MA 02155; and [b]Department of Molecular Genetics and Microbiology, Duke University Medical Center, Durham, NC 27710

Contributed by Thomas D. Petes, October 11, 2013 (sent for review September 10, 2013)

Interstitial telomeric sequences (ITSs) are present in many eukaryotic genomes and are linked to genome instabilities and disease in humans. The mechanisms responsible for ITS-mediated genome instability are not understood in molecular detail. Here, we use a model *Saccharomyces cerevisiae* system to characterize genome instability mediated by yeast telomeric (Ytel) repeats embedded within an intron of a reporter gene inside a yeast chromosome. We observed a very high rate of small insertions and deletions within the repeats. We also found frequent gross chromosome rearrangements, including deletions, duplications, inversions, translocations, and formation of acentric minichromosomes. The inversions are a unique class of chromosome rearrangement involving an interaction between the ITS and the true telomere of the chromosome. Because we previously found that Ytel repeats cause strong replication fork stalling, we suggest that formation of double-stranded DNA breaks within the Ytel sequences might be responsible for these gross chromosome rearrangements.

interstitial telomeres | telomere silencing

The presence of tandem DNA repeats at the ends (telomeres) of chromosomes is essential to protect them from degradation and to maintain genome integrity. The budding yeast *Saccharomyces cerevisiae* telomeres are relatively short (300 ± 75 bp), consisting of repeats of the form $(G_{1-3}T)_n \bullet (AC_{1-3})_n$ (1). Telomeric DNA normally is bound by a multiprotein capping complex that is essential to maintain the integrity of telomeres, protecting them from DNA repair and recombination (1). Proximity to the telomeres may repress transcription, an effect known as the telomere-position effect (1).

In addition to their location at chromosomal termini, telomeric repeats also are present at internal sites of the chromosomes in many organisms (2). Two types of interstitial telomeric sequences (ITSs) are detected in mammalian genomes: heterochromatic ITSs (het-ITSs) and short ITSs (s-ITSs). Het-ITSs are believed to be the remnants of ancestral chromosomal fusions (3) and often colocalize with sites of spontaneous or induced chromosome breakage (4). S-ITSs are believed to represent insertions of telomeric repeats that occur during the repair of double-stranded DNA breaks (5). A subset of s-ITSs in the human genome is bound by the shelterin proteins Rap1, TRF1, and TRF2 (6). In primates and rodents, s-ITSs colocalize with some of the chromosomal fragile sites (7, 8) and map to chromosome breakpoints in cancer cells (9). An 800-bp s-ITS integrated into the intron of the *APRT* gene in Chinese hamster ovary cells substantially increased the rate of deletions and insertions (10).

Although these observations imply that ITSs can trigger a variety of types of genome instability, little is known about their mechanisms. In the present study, we developed a model system to investigate the effect of ITSs on genome stability. We found that interstitial yeast telomeric (Ytel) repeats have very high rates of small-scale expansions and contractions, and trigger gross chromosomal rearrangements (GCRs), including deletions, duplications, inversions, and translocations, as well as the formation of acentric minichromosomes.

Results

System for the Detection of Genome Instabilities Caused by the Ytel Repeats. The reporter gene used to detect changes within the interstitial Ytel sequences is closely related to the one used previously to detect expansions of the $(GAA)_n$ repeats (11), which were inserted into an intron of the artificially split *URA3* gene (construction details are in *SI Methods*, Tables S1 and S2). Because long (>1-kb) introns are inefficiently removed from pre-mRNA in yeast (12), large-scale expansions of the $(GAA)_n$ tracts produce Ura^- clones that might be selected on the medium containing 5-fluoroorotic acid (5-FOA) (11). 5-FOA–resistant clones also resulted from large deletions around those repeats (11, 13), as well as from the repeat-induced mutagenesis in the body of the *URA3* gene (13–15).

To determine whether interstitial telomeric repeats also are subject to expansions and other types of instabilities, a similar *URA3* reporter with these repeats in its intron was inserted into the chromosome III near the active replication origin *ARS306* (Fig. 1 and Fig. S1). The endogenous *URA3* locus on chromosome V contained the mutant *ura3-52* allele. Although the natural yeast telomeres do not have identical copies of a small repeat, we constructed reporter genes that had either 8 or 15 copies of the perfect octameric repeat (TGTGTGGG), which is complementary to the telomeric RNA template within telomerase (16). The $(TGTGTGGG)_n$ sequence was in the nontranscribed strand of *URA3* placing it onto the lagging strand template for replication forks emanating from *ARS306* responsible for replication of our reporter (11). Yeast strains with

Significance

Telomeres are composed of simple repetitive DNA sequences that normally are located at the ends of the chromosomes. Occasionally, however, they also are found inside chromosomes. Some of these internal or interstitial telomeric sequences colocalize with chromosomal fragile sites, preferred sites of breakage in some cancers and hereditary human diseases. The mechanisms responsible for genome instability at interstitial telomeric sequences are unclear. We developed a system to study genetic instabilities caused by these sequences in a model organism (baker's yeast) that allowed us to characterize various chromosomal rearrangements and to measure the likelihood of their formation. We found that interstitial telomeric sequences promote the formation of deletions, duplications, inversions, and translocations, and we proposed molecular mechanisms responsible for these events.

Author contributions: A.Y.A., T.D.P., and S.M.M. designed research; A.Y.A., P.W.G., M.D., A.A.S., and J.C.K. performed research; A.Y.A., P.W.G., M.D., A.A.S., and J.C.K. contributed new reagents/analytic tools; A.Y.A., P.W.G., M.D., A.A.S., J.C.K., T.D.P., and S.M.M. analyzed data; and A.Y.A., T.D.P., and S.M.M. wrote the paper.

The authors declare no conflict of interest.

See Commentary on page 19664.

[1]To whom correspondence may be addressed. E-mail: tom.petes@duke.edu or sergei.mirkin@tufts.edu.

This article contains supporting information online at www.pnas.org/lookup/suppl/doi:10.1073/pnas.1319313110/-/DCSupplemental.

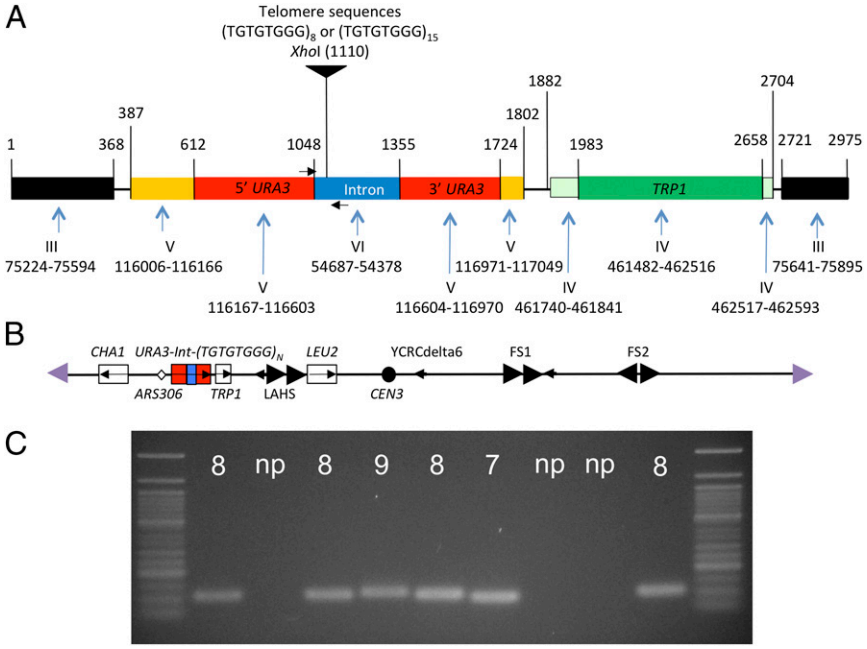

Fig. 1. System used to detect genome instability induced by ITSs. (*A*) Cassette used to generate strains with ITS sequences. The ~3-kb cassette contains flanking sequences from chromosome III (black), flanking and coding sequences from *URA3* (yellow and red, respectively), intronic sequences from the *ACT1* gene (blue), and *TRP1* flanking and coding sequences (pale green and dark green, respectively). Telomeric repeats were inserted into the indicated *XhoI* site within the intron. Small arrows flanking the XhoI site show the positions of primers UIRL1 and UIRL2. Numbers above the cassette indicate the position in the cassette, and numbers below the line are SGD coordinates. (*B*) Location of the cassette on chromosome III showing various relevant chromosome elements. Large black arrows indicate Ty elements and small arrows show solo delta elements; large purple arrows indicate the telomeres. LAHS, FS1, and FS2 are abbreviations for left-arm hotspot, fragile site 1, and fragile site 2 (17). (*C*) Representative PCR analysis of 5-FOA^R colonies derived from strain SMY752 that contained the eight-repeat telomeric tract. Primers located within 50 bp of the insertion were used to amplify genomic DNA, and the resulting fragments were separated by gel electrophoresis. Nos. 7, 8, and 9, the amount of YtelI repeats as confirmed by DNA sequencing; np, no PCR product indicative of genomic rearrangements.

either the $(TGTGTGGG)_8$ or the $(TGTGTGGG)_{15}$ insertions (strains SMY752 and SMY749, respectively) were Ura$^+$ and 5-FOA^S, although a quantitative measurement of gene expression (Fig. S2) indicated that the $(TGTGTGGG)_{15}$ YtelI tract reduced expression of the spliced *URA3* transcript. Because telomeric tracts in the opposite orientation resulted in an even stronger suppression of splicing, we did not attempt a direct comparison of the effects of tract orientation on genome stability.

Interstitial YtelI Repeats Are Naturally Highly Unstable. In the 5-FOA^S strains SMY752 and SMY749, we looked for tract expansions or other gene-inactivating changes by selecting 5-FOA^R derivatives. In the control strain (SMY803) with no YtelI sequences in the reporter, the rate of 5-FOA^R derivatives was about 0.4×10^{-7} per division. This rate was elevated in strains with $(TGTGTGGG)_8$ and $(TGTGTGGG)_{15}$ YtelI tracts 20-fold and 125-fold, respectively (Table 1). The 5-FOA^R derivatives of all three strains initially were examined by PCR analysis with the primers (UIRL1/UIRL2) that flanked the YtelI tracts (Fig. 1*A*). In the control strain, most of the independent derivatives (40 of 42) generated a PCR fragment with these primers. We sequenced five of such derivatives, and all had mutations in the *URA3* coding sequence (Table S3).

For the SMY752 strain (Fig. 1*C*), 24 of 96 derivatives obtained from independent cultures (four derivatives per culture) failed to produce a PCR fragment with primer pairs closely (within 100

Table 1. Rates of genetic alterations observed in 5-FOA^R strains derived from SMY803, SMY752, and SMY749

Strain	Repeat no.	5-FOA^R rate ($\mu \times$ E-07)*	Tract alteration rate ($\mu \times$ E-08)	*ura3* point mutation rate ($\mu \times$ E-07)†	Rate of potential GCR events ($\mu \times$ E-07)‡
SMY803	0 repeats	0.4 (0.2–0.6) [1]	Not applicable	0.3 (0.1–0.5) [1]	0.03 (0.002–0.06) [1]
SMY752	$(TGTGTGGG)_8$	8 (6–10) [20]	5 (1–11)§	8 (4–14) [27]	4 (2–6) [133]
SMY749	$(TGTGTGGG)_{15}$	50 (38–64) [125]	15 (4–29)¶	23 (12–35) [77]	36 (21-53) [1,200]

*The rates of 5-FOA^R derivatives were determined by measuring the frequencies of 5-FOA^R colonies per culture. Rates and 95% confidence intervals (in parentheses) were calculated using the Ma–Sandri–Sarkar maximum likelihood estimator with a correction for sampling efficiency. Numbers in brackets are fold increases relative to rates in SMY803.

†This category includes 5-FOA^R derivatives that had no change in the number of telomeric repeats, as determined by PCR. DNA sequence analysis confirmed that these strains had mutations in the *URA3* sequences flanking the intron.

‡This category includes 5-FOA^R isolates that failed to produce a PCR fragment using primers flanking the telomeric tract.

§Using primers flanking the ITSs, we looked for tract alterations in multiple 5-FOA^R derivatives in independent cultures. Eight small-scale alterations were observed among 96 isolates examined, and all cases represented double events, in which the change in the repeat length was accompanied by a mutation in *URA3*. Because the tract alterations are not responsible for the 5-FOA^R phenotype, the true rate of tract alterations is much higher than indicated for SMY752 and SMY749.

¶Only two single-repeat expansions were observed among about 50 5-FOA^R isolates. Sequencing of one of them showed that the change in the repeat length was accompanied by a mutation in *URA3*.

bp) flanking the tract. As discussed below, these isolates likely contain chromosome rearrangements. Seventy-two derivatives did produce the PCR fragment with the adjacent primers, of which 64 isolates showed no alterations in the repeat length. We sequenced the *URA3* gene from 33 such isolates (from 11 independent cultures) and found that most of them (26 of 33) had mutations in the *URA3* coding sequence (Table S3). In the eight isolates with altered Ytel tracts, four had an addition and four had a deletion of just one repeat. These tract alterations probably were not responsible for the 5-FOA^R phenotype, because the two sequenced isolates of this class had additional mutations in the *URA3* coding sequence in both cases.

In SMY749, we examined 71 5-FOA^R isolates from 24 independent cultures. Of these isolates, 44 lacked a PCR fragment. As described below, we examined 15 of the isolates that lacked the intron-spanning PCR product by other techniques, and all of them had chromosome rearrangements. The remaining 27 isolates had an unchanged Ytel tract. We sequenced five such derivatives: four had alterations in the *URA3* coding sequence, whereas one had a mutation at the intron–exon junction (Table S3).

Because small changes in the number of repeats did not generate a 5-FOA^R strain, we also looked for small expansions or contractions of the $(TGTGTGGG)_{15}$ tract in the nonselective conditions. To this end, 20 clones each from 12 independent cultures grown nonselectively were analyzed by PCR. We detected 11 small-scale tract alterations involving a loss or gain of one to two repeats (Table S4). The calculated rates of alterations (95% confidence limits in parentheses) corresponded to 2.2 (0.7–4.3) $\times 10^{-3}$ per division for expansions and 1.4 (0.4–2.9) $\times 10^{-3}$ per division for contractions.

In summary, our analysis demonstrates that ITSs are associated with several types of instability. First, the tracts gain or lose small numbers of repeats at high rates, whereas large tract expansions were not observed. Second, ITSs stimulate mutations in flanking sequences. Several studies recently showed that double-strand DNA breaks (DSBs) in long $(GAA)_n$ tracts (11, 13–15) or inverted repeats (14) elevate rates of mutations in closely linked genes. It is likely that ITSs operate by related mechanisms. Third, ITSs stimulate GCRs as described below.

Contour-Length Homogeneous Electric Field Gel and Microarray Analyses of GCR Events Induced by YTel Sequences. We examined 15 5-FOA^R derivatives of the SMY749 strain (designated SMY779), in which no PCR fragment was detected with primers flanking the YTel sequences, by a variety of approaches beginning with contour-length homogeneous electric field (CHEF) gel analysis. Intact chromosomal DNA molecules were separated using CHEF gels, transferred to nylon membranes, and hybridized to probes located either centromere-proximal (*LEU2*) or centromere-distal (*CHA1*) to our *URA3* reporter. Four patterns were observed. In seven isolates (nos. 1, 9, 17, 18, 20, 24, and 27), chromosome III was identical in size to the original chromosome III (about 365 kb), and both probes hybridized to the same chromosome (Fig. 2). We refer to this class as class 1. In the single class 2 strain (no. 4), chromosome III was about 10 kb smaller than the original chromosome III, but still hybridized to both the *LEU2* and *CHA1* probes. Seven isolates had no DNA fragment similar in size to the original chromosome III. In six of them (nos. 7, 10, 11, 19, 21, and 25), the *LEU2* probe hybridized to chromosomes that varied in size from about 435–490 kb, whereas the *CHA1* probe hybridized to a DNA fragment of ~80 kb (Fig. 2*C*), which is smaller than any of the yeast chromosomes (class 3). In the remaining isolate, designated class 4 (no. 12), the *LEU2* probe hybridized with a chromosome of ~290 kb, and the *CHA1*-hybridizing fragment was ~80 kb long.

The same DNA samples then were examined by comparative genome hybridization (CGH) microarray (17). Deletions or duplications of single-copy regions ≥5 kb throughout the genome

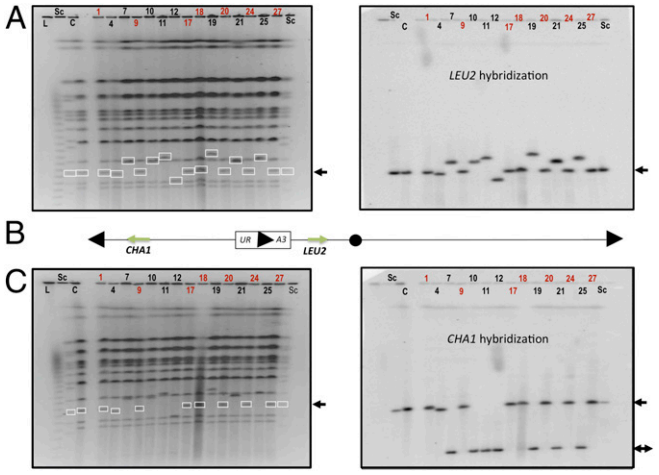

Fig. 2. CHEF gel analysis of chromosome rearrangements in 5-FOA^R isolates of SMY749 that had alterations in the sequences flanking the ITS. (*A*) Chromosomal DNA from 15 isolates was compared with DNA from the SMY749 control strain (lane C). Lanes labeled "L" and "Sc" contain size standards (Bio-Rad), catenated lambda bacteriophage chromosome and yeast chromosomes from a standard laboratory strain, respectively. The gel was stained with ethidium bromide (*Left*) and subsequently transferred to nitrocellulose filters and hybridized to *LEU2* (*Right*). The positions of the hybridizing bands in the ethidium bromide-stained gel are boxed, and arrows show the position of chromosome III before the chromosome rearrangement. (*B*) Locations of the hybridization probes relative to the *URA3::Ytel* gene. (*C*) CHEF electrophoresis followed by Southern analysis using the *CHA1* hybridization probe. The minichromosome is shown by a double arrow on the right side of the figure.

can be detected readily. Fig. 3 shows CGH data for chromosome III of the four classes described above. In class 1 isolates, no deletions or duplications on chromosome III or any other yeast chromosome were observed. In class 2 isolates, there is a deletion of ~10 kb that removed sequences from the *URA3::Ytel* reporter gene to a Ty1 element of left arm transposition hotspot (LAHS) (Fig. 1*B*). Two class 3 isolates have the same 10-kb deletion as in class 2, but also have a duplication of sequences derived from the right arm of chromosome III ranging from ~190 kb in no. 11 to ~215 kb in no. 19. The starting point of these duplications is near *YCRCdelta6* in no. 11 and near the Ty/delta elements of fragile site 1 (FS1) in no. 19 (Fig. 1*B*). In the class 4 isolate (no. 12), chromosome III has the same 10-kb deletion as above plus a duplication of 30-kb DNA segment located at the left telomere of chromosome II starting near *YBLWTy2-1* (Fig. S3*B*).

Both class 3 and 4 strains have an 80-kb minichromosome that hybridizes to the *CHA1* probe. To identify the sequences within this minichromosome, we purified it from a CHEF gel and hybridized it to the CGH arrays. As shown in Fig. 3, it contains all the chromosome III sequences between the left telomere and *URA3::Ytel* reporter.

Inversions Between Interstitial and Terminal Telomeric Repeats in Class 1 Strains. Unlike the class 2–4 strains, class 1 strains did not have detectable deletions or duplications. Using PCR analysis and Southern analysis (*SI Methods*, Fig. S4), we found that class 1 strains do have a rearrangement on chromosome III, which is an 80-kb–long inversion of the chromosomal segment between the interstitial Ytel repeat and the natural telomere. Fig. 4 shows that in class 1 strains, a PCR fragment may be generated with a primer located within the 3′ part of the *URA3* reporter and a primer located near the left telomere. The size of the resulting PCR product varies, because the length of telomeric DNA is different in different isolates. Based on the size of this fragment, the approximate lengths in base pairs of the

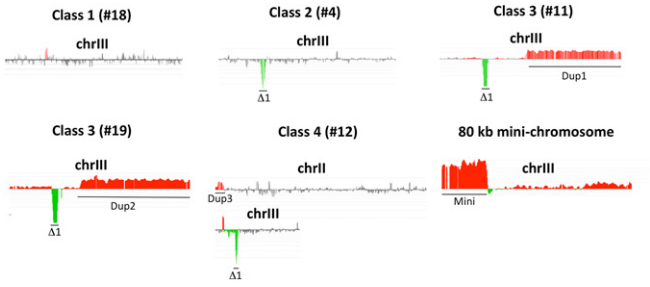

Fig. 3. CGH microarray analysis of 5-FOA^R derivatives of SMY749. The results of CGH experiments analyzed with the CGH-Miner program. Genomic DNA isolated from the experimental strain was labeled with Cy5-dUTP, DNA from the control strain without chromosome rearrangements (SMY749) was labeled with Cy3-dUTP, and the samples were mixed and hybridized to microarrays containing all ORFs and intergenic regions. The horizontal line represents the entire length of chromosome III (or II). Green and red show a significant deletion or duplication of sequences, respectively. The approximate SGD coordinates for the labeled deletions and duplications on the indicated chromosomes are Δ1 (III, 76,000–85,000), Dup1 (III, 150,000-right telomere), Dup2 (III, 125,000-right telomere), Dup3 (II, 1–30,000), and Mini (III, 1–76,000). The number of the 5-FOA^R isolate is shown in parentheses. The CGH analysis of the minichromosome was done using a chromosome purified from a CHEF gel.

interstitial telomeric DNA after the inversion in different isolates varies between 315 and 540 bp. We also sequenced part of the PCR product containing the ITS in the class 1 strain SMY779-#27. The first 60 bp of the ITS adjacent to the X repeat (Fig. 4*A*) were identical to the telomeric sequences adjacent to the X repeat in the *Saccharomyces* Genome Database (SGD), whereas the sequences at the other junction were six perfect repeats of TGTGTGGG. These results are consistent with the model proposed in Fig. 4*A*.

Class 2–4 strains were Trp$^-$ because the 10-kb deletion associated with the chromosome rearrangement removed the *TRP1* gene located adjacent to the *URA3::Ytel* gene. Unexpectedly, however, class 1 strains were Trp$^-$ as well. Long yeast telomeric repeats located internally on the chromosome have been shown to repress expression of nearby genes (18, 19), and this Rap1- and Sir2-dependent telomeric silencing (1) is reversed by nicotinamide (20). Because class 1 strains had Ytel repeats that were at least twice as long as the original strain without the chromosome rearrangement (120 bp), we hypothesized that the Trp$^-$ phenotype reflected telomeric silencing. Consistent with this possibility, we found that Rap1p is recruited to the Ytel repeats and the flanking *URA3* sequences by chromatin immunoprecipitation (Fig. S5). Furthermore, class 1 strains grown in the presence of nicotinamide have Trp$^+$ phenotype (Fig. S6). Thus, chromosome rearrangements induced by ITS sequences may affect gene expression as well as chromosome structure.

Discussion

Genetic instabilities caused by DNA microsatellites have been studied for several decades in connection with hereditary human diseases, cancer, and chromosomal fragility. The effects of multiple types of microsatellites, particularly trinucleotide repeats, on genome stability have been investigated in detail in *S. cerevisiae.* In yeast, certain microsatellites [such as $(CTG)_n$ and $(GAA)_n$] may act as hotspots for mitotic DSBs that are recombinogenic and/or associated with chromosome rearrangements (21, 22).

From our analysis of ITSs, it is clear that some of the genome-destabilizing effects of these sequences are shared with other types of microsatellites. In strains with the $(TGTGTGGG)_{15}$ repeats, deletions and additions of one repeat were remarkably frequent, about 10^{-3} per cell division. For comparison, deletions and additions of repeats in a $(CAATCGGT)_{10}$ tract occurs at a rate of about 10^{-5} per division (23). Of the 5-FOA^R isolates derived from SMY752 and SMY749, none had large expansions. In contrast, large expansions were the main class leading to 5-FOA resistance for $(GAA)_n$ tracts longer than 100 repeats.

Mutations in the coding sequence of the *URA3::Ytel* reporter were substantially (>20-fold) induced by both the 8- and 15-copies of Ytel tracts (Table 1). Similar induction of mutagenesis was observed for $(GAA)_n$ and inverted repeats [repeat-induced mutagenesis (RIM)] (11, 13–15). All these repeats stall the replication fork progression (24–26), and the $(TGTGTGGG)_{15}$ run is a particularly potent replication block. A connection between stalled replication forks and DSBs in yeast also has been observed for CTG repeats (22) and in *mec1* cells treated with hydroxyurea (27). The recombinogenic repair of DSBs is known to be error prone (28), and single-stranded DNA recombination intermediates are particularly susceptible to mutations (29). We believe, therefore, that error-prone DSB repair might be responsible for RIM.

In about half the 5-FOA^R derivatives of the *URA3::Ytel* strains, we detected no PCR fragments using primers flanking the telomeric tract. The rate of formation of these strains was elevated about 100-fold by the $(TGTGTGGG)_8$ tract and about 1,000-fold by the $(TGTGTGGG)_{15}$ tract. All these strains contained chromosome rearrangements that were consistent with a DSB within the ITS as their initiating event; these breaks, however, have not been demonstrated by direct physical methods.

In class 1 strains, we suggest that the broken ends generated by the DSB within the ITS are processed by exonucleases (30) to yield a protruding 3′ G-rich single strand on the 80-kb acentric chromosome fragment, and a protruding C-rich single strand on the centromere-containing fragment (Figs. 4*A* and 5*A*). The protruding C-rich single strand of the centromere-containing fragment might anneal with the left telomere (which has a protruding G-rich strand) to produce the observed inversion. This event would split the *URA3* cassette into two noncontiguous fragments, resulting in the 5-FOA^R phenotype. Although a similar structure might be produced by a mechanism in which two broken chromatids anneal to produce one chromosome with an inversion, similar to a half-crossover, we prefer the model shown in Fig. 4*A*, because half-crossovers usually are observed only in strains defective in homologous recombination (31).

By the model shown in Fig. 4*A*, the telomeres derived from the ITS sequence would have a maximum length of 120 bp. From Southern analysis of class 1 strains (Fig. S4*C*), we calculated that the newly formed telomeres in class 1 strains are about 360 bp, similar in length to telomeres in wild-type strains (1). These results suggest that telomerase extended the telomeric repeats associated with the 5′ end of the reporter gene.

The single class 2 strain had a deletion on chromosome III that removes the intron with Ytel sequences and the 3′ end of the *URA3* reporter, as well as all sequences between the *URA3* reporter up to the Watson-oriented Ty element on the left arm; the 5′ portion of the reporter gene was retained. By PCR analysis, followed by DNA sequencing, we identified the junction between the 5′ portion of *URA3* and the Ty element on chromosome III as identical to the junction between the *URA3* coding sequence and Ty sequences of the *ura3-52* allele on chromosome V (32). This observation is consistent with the model, in which one end of the DSB within the ITS sequence is degraded into the 5′ part of the *URA3::Ytel* reporter, whereas its other end is degraded into the Ty element of LAHS. The two ends then invade the *ura3-52* allele, and the subsequent gene conversion event would yield the class 2 rearrangement (Fig. 5*B*).

Class 3 and 4 events reflect similar mechanisms (Fig. 5 *C* and *D*) likely initiated by a DSB within the ITS. Because classes 3 and 4 have 80-kb minichromosomes, this acentric fragment does not recombine with other yeast sequences. Note that the broken end of this acentric fragment has the structure required for a

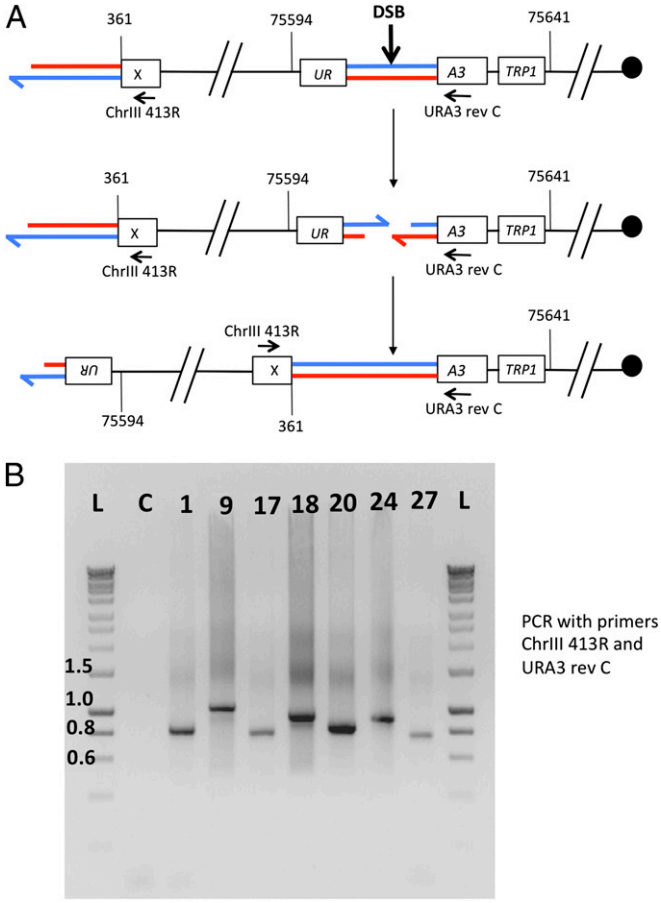

Fig. 4. Formation and analysis of class 1 events (terminal inversions). (*A*) Mechanism for inversion (see text for details). Telomeric repeats are shown as double-stranded DNA molecules, with blue and red indicating the GT-rich and CA-rich strands, respectively. The rectangle labeled "X" indicates the conserved subtelomeric X repeat (1), and the horizontal arrows show the positions of primers used to diagnose the inversion. (*B*) PCR analysis of class 1 events.

functional telomere: the 3′ end has $G_{1-3}T$ sequences. In the centromere-containing fragment, however, the orientation of the telomeric repeats (3′ end with $C_{1-3}A$ sequences) is in an orientation precluding telomere formation. We term such sequences "reverse-telomeres." For the centromere-containing fragment to form a stable chromosome, this reverse-telomere sequence must be removed and replaced by a functional telomere. Thus, the reverse-telomeres are degraded until the Ty sequences in the LAHS are rendered single stranded, the resulting end invades Ty or delta elements on the right arm of the chromosome, and sequences distal to the point of invasion are then copied by break-induced replication (BIR).

The single class 4 event likely is generated by a mechanism similar to class 3, except the processed centromere-containing fragment invades a Ty element located on chromosome II, which results in a BIR event extending from the point of invasion to the left end of chromosome II (Fig. 5*D*). Indeed, GCRs caused by recombination between Ty or delta elements were observed in many previous studies in yeast (33, 34).

Because the 80-kb minichromosome is acentric, it would be expected to be very unstable. As this minichromosome contains essential genes, cells that lose it would not be viable, which should reduce the growth rate of the corresponding strains substantially, yet class 3 strains formed colonies that were only slightly smaller than a control strain (Fig. S7). We hypothesize that some sequence on this minichromosome might have a centromere-like activity, or that the segregation of the minichromosome is coupled to the segregation of other chromosomes (35). Paek et al. (36) previously used PCR to demonstrate acentric fragments in yeast generated by template switching during DNA replication, although the stability of these fragments could not be quantitated.

All four classes of genome rearrangements are explained readily as the outcomes of a DSB repair within the ITS. A DSB at this position likely is caused by the very potent replication block observed in strains with the $(TGTGTGGG)_{18}$ tract (24), because DSBs were observed previously at stalled replication forks in yeast (22, 27). The latter likely is the result of a tight nucleoprotein complex formed at the interstitial Ytel sequences. We show here that the telomere-binding Rap1 protein covers the interstitial Ytel sequence (Fig. S5). Furthermore, fork stalling at ITSs decreases dramatically if we knock out Tof1 protein (24), which is known to preserve protein-mediated replication blocks (37).

In summary, we observed that interstitial telomeric repeats are potent sources of genome instability and unraveled molecular mechanisms of those events. An unexpected payback from this

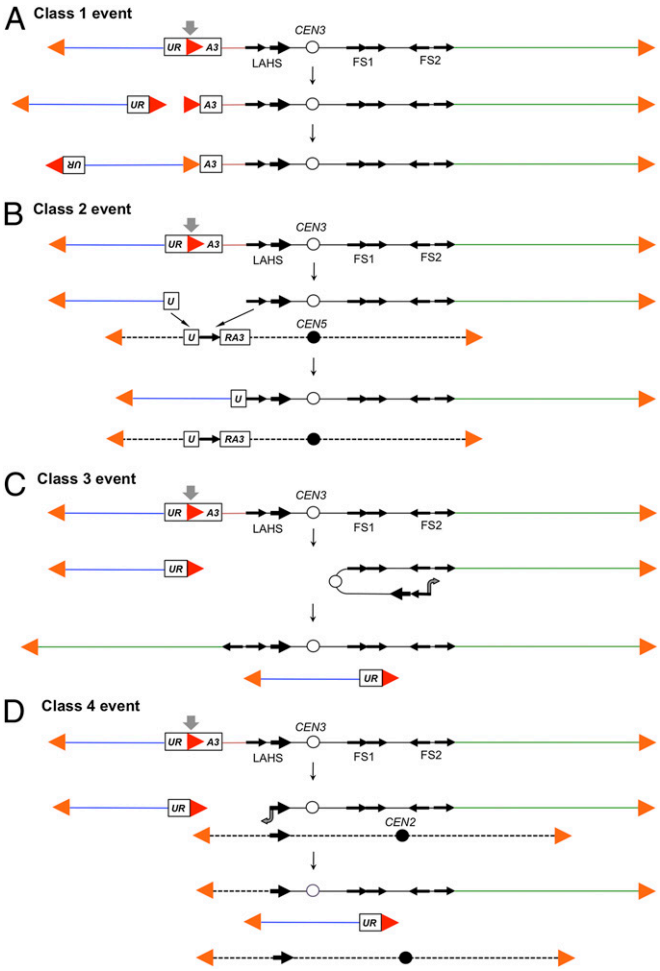

Fig. 5. Mechanisms responsible for four classes of chromosomal rearrangements (see text for details). (*A*) Terminal inversion (class 1). (*B*) Deletion associated with gene conversion (class 2). (*C*) Deletion/duplication of chromosome III and minichromosome (class 3). (*D*) Translocation and minichromosome (class 4). ITSs are shown as red triangles, telomeric repeats at chromosome ends are shown as orange triangles, centromeres are shown as circles (white for chromosome III and black for other chromosomes), and Ty and delta elements are shown as black arrows.

analysis is that the *URA3*::*Ytel* reporter may be used as a tool to generate chromosomes of desired sizes.

Methods

Yeast Strains. We used three isogenic haploid strains with an intron-containing *URA3* gene on chromosome III: SMY803 (no telomeric repeats), SMY752 (URA3::Ytel with eight telomeric repeats), and SMY749 (URA3::Ytel with 15 repeats). (See *SI Methods* for details.)

Measurements of the Rates of Gene-Inactivating Events. Strains with the starting *URA3-Int* cassettes are Ura$^+$ and, thus, sensitive to the 5-FOA. For each strain, we determined the frequencies of 5-FOA^R derivatives in multiple independent cultures and converted those data into rate estimates (details in *SI Methods*). Genomic DNA samples from individual 5-FOA^R isolates were examined by PCR using primers flanking the intron (UIRL1/ UIRL2 or 1829F/ 1829R). This analysis indicated whether the number of telomeric repeats had changed in those isolated or whether they contained chromosome rearrangements. Some of the isolates with an unaltered tract were sequenced to detect point mutations in the body of the *URA3* cassette (*SI Methods*).

Analysis of Chromosome Rearrangements. The 5-FOA^R derivatives of SMY749 that did not produce a PCR fragment containing Ytel repeats were examined for chromosome rearrangements using CHEF gel electrophoresis and CGH microarrays (*SI Methods*). For some of these derivatives, the rearrangement breakpoints were analyzed by standard Southern analysis and PCR (Fig. S3 and Table S5).

ACKNOWLEDGMENTS. We thank K. Bloom, D. Gottschling, J. Rine, and members of the S.M.M. and T.D.P. laboratories for useful discussions; Gil Han for technical support; and Durwood Marshall from Tufts University Information Technology, Research and Geospatial Technology Services for statistical consulting. The research was supported by National Institutes of Health Grant GM60987 (to S.M.M.) and Grants GM52319 and GM24110 (to T.D.P.).

1. Wellinger RJ, Zakian VA (2012) Everything you ever wanted to know about Saccharomyces cerevisiae telomeres: Beginning to end. *Genetics* 191(4):1073–1105.
2. Ruiz-Herrera A, Nergadze SG, Santagostino M, Giulotto E (2008) Telomeric repeats far from the ends: Mechanisms of origin and role in evolution. *Cytogenet Genome Res* 122(3-4):219–228.
3. Slijepcevic P (1998) Telomeres and mechanisms of Robertsonian fusion. *Chromosoma* 107(2):136–140.
4. Slijepcevic P, Xiao Y, Dominguez I, Natarajan AT (1996) Spontaneous and radiation-induced chromosomal breakage at interstitial telomeric sites. *Chromosoma* 104(8): 596–604.
5. Nergadze SG, Santagostino MA, Salzano A, Mondello C, Giulotto E (2007) Contribution of telomerase RNA retrotranscription to DNA double-strand break repair during mammalian genome evolution. *Genome Biol* 8(12):R260.
6. Simonet T, et al. (2011) The human TTAGGG repeat factors 1 and 2 bind to a subset of interstitial telomeric sequences and satellite repeats. *Cell Res* 21(7):1028–1038.
7. Ruiz-Herrera A, et al. (2005) Evolutionary breakpoints are co-localized with fragile sites and intrachromosomal telomeric sequences in primates. *Cytogenet Genome Res* 108(1-3):234–247.
8. Camats N, et al. (2006) Genomic instability in rat: Breakpoints induced by ionising radiation and interstitial telomeric-like sequences. *Mutat Res* 595(1-2):156–166.
9. Lin KW, Yan J (2008) Endings in the middle: Current knowledge of interstitial telomeric sequences. *Mutat Res* 658(1-2):95–110.
10. Kilburn AE, Shea MJ, Sargent RG, Wilson JH (2001) Insertion of a telomere repeat sequence into a mammalian gene causes chromosome instability. *Mol Cell Biol* 21(1): 126–135.
11. Shishkin AA, et al. (2009) Large-scale expansions of Friedreich's ataxia GAA repeats in yeast. *Mol Cell* 35(1):82–92.
12. Yu X, Gabriel A (1999) Patching broken chromosomes with extranuclear cellular DNA. *Mol Cell* 4(5):873–881.
13. Tang W, Dominska M, Gawel M, Greenwell PW, Petes TD (2013) Genomic deletions and point mutations induced in Saccharomyces cerevisiae by the trinucleotide repeats (GAA·TTC) associated with Friedreich's ataxia. *DNA Repair (Amst)* 12(1):10–17.
14. Saini N, et al. (2013) Fragile DNA motifs trigger mutagenesis at distant chromosomal loci in saccharomyces cerevisiae. *PLoS Genet* 9(6):e1003551.
15. Shah KA, et al. (2012) Role of DNA polymerases in repeat-mediated genome instability. *Cell Rep* 2(5):1088–1095.
16. Singer MS, Gottschling DE (1994) TLC1: Template RNA component of Saccharomyces cerevisiae telomerase. *Science* 266(5184):404–409.
17. Lemoine FJ, Degtyareva NP, Lobachev K, Petes TD (2005) Chromosomal translocations in yeast induced by low levels of DNA polymerase a model for chromosome fragile sites. *Cell* 120(5):587–598.
18. Gottschling DE, Aparicio OM, Billington BL, Zakian VA (1990) Position effect at S. cerevisiae telomeres: Reversible repression of Pol II transcription. *Cell* 63(4): 751–762.
19. Stavenhagen JB, Zakian VA (1994) Internal tracts of telomeric DNA act as silencers in Saccharomyces cerevisiae. *Genes Dev* 8(12):1411–1422.
20. Bitterman KJ, Anderson RM, Cohen HY, Latorre-Esteves M, Sinclair DA (2002) Inhibition of silencing and accelerated aging by nicotinamide, a putative negative regulator of yeast sir2 and human SIRT1. *J Biol Chem* 277(47):45099–45107.
21. Kim HM, et al. (2008) Chromosome fragility at GAA tracts in yeast depends on repeat orientation and requires mismatch repair. *EMBO J* 27(21):2896–2906.
22. Freudenreich CH, Kantrow SM, Zakian VA (1998) Expansion and length-dependent fragility of CTG repeats in yeast. *Science* 279(5352):853–856.
23. Sia EA, Kokoska RJ, Dominska M, Greenwell P, Petes TD (1997) Microsatellite instability in yeast: Dependence on repeat unit size and DNA mismatch repair genes. *Mol Cell Biol* 17(5):2851–2858.
24. Anand RP, et al. (2012) Overcoming natural replication barriers: Differential helicase requirements. *Nucleic Acids Res* 40(3):1091–1105.
25. Voineagu I, Narayanan V, Lobachev KS, Mirkin SM (2008) Replication stalling at unstable inverted repeats: Interplay between DNA hairpins and fork stabilizing proteins. *Proc Natl Acad Sci USA* 105(29):9936–9941.
26. Krasilnikova MM, Mirkin SM (2004) Replication stalling at Friedreich's ataxia (GAA)n repeats in vivo. *Mol Cell Biol* 24(6):2286–2295.
27. Feng W, Di Rienzi SC, Raghuraman MK, Brewer BJ (2011) Replication stress-induced chromosome breakage is correlated with replication fork progression and is preceded by single-stranded DNA formation. *G3 (Bethesda)* 1(5):327–335.
28. Malkova A, Haber JE (2012) Mutations arising during repair of chromosome breaks. *Annu Rev Genet* 46:455–473.
29. Yang Y, Sterling J, Storici F, Resnick MA, Gordenin DA (2008) Hypermutability of damaged single-strand DNA formed at double-strand breaks and uncapped telomeres in yeast Saccharomyces cerevisiae. *PLoS Genet* 4(11):e1000264.
30. Symington LS, Gautier J (2011) Double-strand break end resection and repair pathway choice. *Annu Rev Genet* 45:247–271.
31. Haber JE, Hearn M (1985) Rad52-independent mitotic gene conversion in Saccharomyces cerevisiae frequently results in chromosomal loss. *Genetics* 111(1):7–22.
32. Rose M, Winston F (1984) Identification of a Ty insertion within the coding sequence of the S. cerevisiae URA3 gene. *Mol Gen Genet* 193(3):557–560.
33. Mieczkowski PA, Lemoine FJ, Petes TD (2006) Recombination between retrotransposons as a source of chromosome rearrangements in the yeast Saccharomyces cerevisiae. *DNA Repair (Amst)* 5(9-10):1010–1020.
34. Chan JE, Kolodner RD (2011) A genetic and structural study of genome rearrangements mediated by high copy repeat Ty1 elements. *PLoS Genet* 7(5):e1002089.
35. Liu YT, Ma CH, Jayaram M (2013) Co-segregation of yeast plasmid sisters under monopolin-directed mitosis suggests association of plasmid sisters with sister chromatids. *Nucleic Acids Res* 41(7):4144–4158.
36. Paek AL, et al. (2009) Fusion of nearby inverted repeats by a replication-based mechanism leads to formation of dicentric and acentric chromosomes that cause genome instability in budding yeast. *Genes Dev* 23(24):2861–2875.
37. Hodgson B, Calzada A, Labib K (2007) Mrc1 and Tof1 regulate DNA replication forks in different ways during normal S phase. *Mol Biol Cell* 18(10):3894–3902.